0026-895X/86/030250-08$02.00/0

MOLECULAR PHARMACOLOGY, 29:250-257

Molecular Mechanisms of the Potent and Stereospecific Nicotinic Receptor Agonist (+)-Anatoxin-a

K. L. SWANSON, C. N. ALLEN, R. S. ARONSTAM, H. RAPOPORT, and E. X. ALBUQUERQUE

Department of Pharmacology and Experimental Therapeutics, University of Maryland School of Medicine, Baltimore Maryland 21201 (K.L.S., C.N.A., E.X.A.), Department of Pharmacology and Toxicology, Medical College of Georgia, Augusta, Georgia 30912 (R.S.A.), and Department of Chemistry, University of California, Berkeley, California 94720 (H.P.)

Received August 13, 1985; Accepted December 13, 1985

SUMMARY

Anatoxin-a (AnTX) was shown to be a highly potent and stereospecific agonist at nicotinic synapses in frog skeletal muscle and *Torpedo* electric organs. AnTX binds to the nicotinic-acetylcholine receptor with a higher affinity than for acetylcholine (ACh) but does not bind to sites in the receptor-gated ionic channel. (+)AnTX caused receptor desensitization, i.e., the loss of agonist-stimulated binding of histrionicotoxin to an allosteric site with time, at a rate significantly slower than that of ACh. Single channel patch clamp recordings indicated that the conductance of channels activated by (+)AnTX (28 pS) and ACh (27 pS) were similar. The (+)AnTX-activated channels contained rapid closing events, the burst times caused by the toxin were shorter than those caused by ACh but had similar voltage dependencies, and the number of short closures per burst was constant at all potentials with both agonists. The bursts of rapid openings and rapid closures (τ = 0.4 msec) appear to result from repetitive opening and closing of the (+)AnTX-bound receptor-ion channel. It is concluded that the semirigid molecule and secondary amine (+)AnTX is a more potent agonist than ACh or carbamylcholine because of a higher affinity for the receptor. At various concentrations the toxin activates the appearance of channels with the same conductances as ACh-induced channels but with a shorter channel lifetime.

(+)AnTX is a potent nicotinic agonist isolated from the blue green algae, *Anabaena flos-aquae* (Refs. 1–3; Fig. 1.). This toxin is produced in fresh water algal blooms and is responsible for the death of livestock and waterfowl via a depolarizing blockade of neuromuscular transmission and subsequent respiratory paralysis (4). In skeletal muscle, when AChE was blocked, the racemic (±)AnTX elicited contracture with a potency similar to that of ACh (5), but with a 10-fold greater potency than that of Carb or succinylcholine (6). (±)AnTX also potentiated nerve-evoked muscle twitches *in vivo* (5) and *in vitro* (6). The toxin competitively inhibited the binding of ACh and (+)-tubocurarine to the nicotinic receptor from *Torpedo* electric organ and enhanced the binding of noncompetitive antagonists phencyclidine and H_{12}-HTX (7). In addition, (±)AnTX acted upon muscarinic and nicotinic receptors located at the ganglionic synapses of the guinea pig ileum (5). Higher concentrations of the toxin were necessary (ED_{50} = 100 μM) to antagonize quinuclidinyl benzilate binding to brain muscarinic receptors (7).

This research was supported by United States Army Medical Research and Development Command Contract DAMD 17-84-C-4219 and Army Research Office Grant DAAG 29-85-K-0090.

AnTX fits geometric models of nicotinic agonists, which suggests that a hydrogen bond forms to a planar region of the agonist (8, 10), and a bulky cationic (charged alkylammonium) group approximately 5.9 Å from the hydrogen bond (Fig. 1) sterically activates the receptor complex (8, 9). Although a secondary amine, the toxin is mostly protonated in solution (pK_a = 9.4; Ref. 3). The bicyclic structure exists primarily with the seven-membered ring in the twist-chair conformation and with the *s-cis* enone conformation favored 3:1 over the *s-trans* conformation because of less steric crowding (3). The *s-cis* conformation is also suggested to be the preferred agonist conformation because of the optimal distance between the quaternized nitrogen and the carbonyl oxygen (Fig. 1). In addition, stereospecificity is evidenced by a greater potency of the natural form (+)AnTX than (−)AnTX at inducing contractures of frog rectus abdominis muscle (suggested in Refs. 11 and 12, and confirmed here).

The present study was undertaken to gain further insights into the molecular interactions of (+)AnTX and (−)AnTX with ACh receptors. The availability of (+)- and (−)AnTX of greater than 99% purity allowed us to correlate their contracture potencies with their ACh receptor binding affinities. The

ABBREVIATIONS: (+)AnTX, (+)-anatoxin-a; (−)AnTX, (−)-anatoxin-a; AChE, acetylcholinesterase; ACh, acetylcholine; Carb, carbamylcholine; H_{12}-HTX, perhydrohistrionicotoxin; HEPES, *N*-2-hydroxyethylpiperazine-*N'*-2-ethanesulfonic acid; DFB, diisopropylfluorophosphate; BGT, α-bungarotoxin.

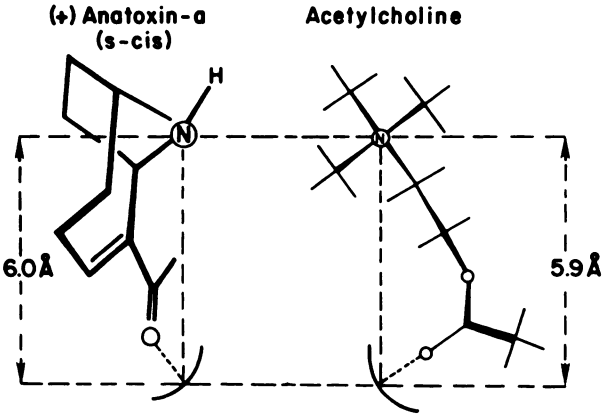

Fig. 1. Comparison of the structures of *s-cis*-(+)AnTX and ACh. The ACh receptor is believed to have a hydrogen-bonding moiety. In ACh, the distance from the nitrogen to the van der Waals radius (1.4 Å) of carbonyl oxygen is 5.9 Å (9). For AnTX in the twist-chair, *s-cis* conformation, the distance to the van der Waals radius of the hydrogen bond is 6.0 Å (3).

extremely high potency of (+)AnTX along with its free access as a secondary amine to the central nervous system and its lack of susceptibility to hydrolysis by AChE enhanced our interest in this neurotoxin.

Materials and Methods

Solutions and drugs. Ringer's solution consisted of (mM): NaCl, 116; KCl, 2.0; $CaCl_2$, 1.8; Na_2HPO_4, 1.3; NaH_2PO_4, 0.7. HEPES-buffered solution consisted of (mM): NaCl, 115; KCl, 2.5; $CaCl_2$, 1.8; and HEPES, 3, adjusted to pH 7.1 with NaOH.

Potency assay. Contracture of frog (*Rana pipiens*) rectus abdominis muscle was used to assay agonist potency. The isolated muscle was separated into halves, and each was mounted in a bath containing frog Ringer's solution and connected to a force transducer with 1 g of resting tension. After 1 hr of equilibration, the testing of contractures began. Some muscles were treated with 1 mM DFP (Calbiochem) for 30 min to inhibit AChE and then were washed for 1 hr to remove free DFP (13, 14). Each agonist application was allowed to contract the muscle for 5 min or until a maximal contraction was reached, whichever was shorter. The muscle was washed five times in 5 min and then at 10-min intervals. Maximal contracture was determined at the end of each experiment using 100 mM K^+ Ringer's solution. Carb and ACh were each assayed at three concentrations, both before and after DFP treatment. Carb, (+)AnTX, and (−)AnTX were assayed at three concentrations each; half of each muscle was treated with DFP and the other half was not. Agonist concentrations which induced only partial contractures were used in order to minimize desensitization. Preliminary experiments verified that repeated doses elicited similar responses and desensitization was minimal. Statistical evaluation of relative potency was according to the method of Colquhoun (15).

Tissue preparation. Electric organs from *Torpedo californica* were purchased from Pacific Biomarine and stored at −70° for up to 4 months before use. To prepare membranes, the electric organ was minced and then homogenized using a Waring blender (maximum speed for 30 sec) in 20 volumes of 50 mM Tris-Cl, pH 7.4, containing 1 mM phenylmethylsulfonyl fluoride and 100 μM DFP to inhibit proteolytic activity and AChE. After filtration through four layers of cheesecloth, the suspension was spun at 15,000 × *g* for 20 min. The pellets were resuspended in buffer and used without further treatment. Protein content was estimated by the method of Lowry *et al.* (16) using bovine serum albumin as the standard.

Binding assays. Nicotinic receptor binding was measured using [^{125}I]BGT (New England Nuclear). *Torpedo* membranes (5–12 μg of protein) were incubated with 5 nM [^{125}I]BGT in 50 mM Tris-Cl, pH 7.4, in a final volume of 1 ml for 20 min at room temperature. The binding reaction was quenched by addition of 0.5 ml of 10 mg/ml methylated bovine serum albumin (Sigma Chemical Co.) followed immediately by filtration through glass fiber filters (Whatman GF/B) which had been soaked in the albumin solution. After washing twice with 5 ml of buffer, the radioactivity content of the filters was determined by liquid scintillation counting. Nonspecific binding was determined in the presence of 100 μM nicotine. The ability of (+)- and (−)AnTX and ACh to compete with [^{125}I]BGT for nicotinic receptor binding sites was determined by incubating the membranes with the agonist for 15 min before adding the [^{125}I]BGT.

Ion channel binding was measured using [^{3}H]H_{12}-HTX (54.5 Ci/mol, prepared as described in Ref. 17) as a probe. To measure equilibrium ion channel binding, *Torpedo* membranes (25–50 μg of protein) were incubated with various concentrations of agonists and 2 nM [^{3}H]H_{12}-HTX for 60 min at room temperature in 50 mM Tris-Cl, pH 7.4, in a final volume of 1 ml. Nonspecific binding was determined in the presence of 10 μM phencyclidine (18). The suspension was then filtered on glass fiber filters (Whatman GF/B) which had been treated with a 1% organosilane solution (Sigmacote, Sigma Chemical Co.) to eliminate [^{3}H]H_{12}-HTX binding to the filters. The filters were washed twice with 5 ml of Tris buffer, and their radioactivity content was determined by liquid scintillation counting.

Receptor ligands, especially agonists, enhance the binding of ion channel probes such as [^{3}H]H_{12}-HTX by increasing the affinity of the receptor complex for the probe by rendering the binding site more accessible to the probe (7, 17, 19, 20). To measure this allosteric "activation," (+)- and (−)AnTX and ACh were added to the *Torpedo* membranes at the same time as the [^{3}H]H_{12}-HTX. Binding was then determined by filtration after a 60-sec incubation. This short incubation period was chosen to minimize desensitization effects. If *Torpedo* membranes were incubated with receptor agonists for a period of time before ion channel binding was assayed, the level of [^{3}H]H_{12}-HTX binding was decreased compared to the situation in which agonist and channel probe were added simultaneously (19). This condition of diminished ion channel binding affinity is thought to be associated with the assumption of a desensitized conformation by the nicotinic receptor complex. To compare the abilities of (+)AnTX and ACh to produce this desensitization, *Torpedo* membranes were incubated with 10 μM AnTX or ACh for 0–5 min before addition of [^{3}H]H_{12}-HTX (final concentration, 2 nM). Binding was then determined by filtration 60 sec later.

Isolation of muscle fibers for patch clamping. Interosseal muscles were dissected from the longest toe of the hindfoot of the frog *R. pipiens* in standard Ringer's solution. The procedure for isolation of single fibers was reported previously (21). Briefly, the muscles were incubated in 1 mg/ml of collagenase (type I, Sigma; 2 hr, 21°) and then in 0.2 mg/ml of protease (type BII, Sigma; 12–20 min) with mild agitation. Fibers were stored in bovine serum albumin (0.3–0.5 mg/ml) and used within 24 hr. Tetrodotoxin (300 nM; Sankyo Labs) was added to all solutions used in patch clamp studies to prevent contraction of the muscle fibers.

Electrophysiological techniques. Microelectrodes of borosilicate capillary glass were pulled in two stages and heat polished to yield micropipettes with resistance of 8–12 MΩ. ACh and AnTX were diluted in HEPES-buffered solution and filtered through a Millipore filter before filling the micropipette. The recording bath was filled with HEPES-buffered solution and maintained at 10°. Gigaohm seals between the nonjunctional surface of the fiber membrane and the microelectrode were formed using standard technique. Patch clamp currents from cell-attached patches were monitored using an LM-EPC-7 instrument (List Electronics). The signal was filtered with a Bessel filter at 3 KHz and recorded on FM magnetic tape for later analysis.

For computer analysis, the signal was filtered at 2 KHz with a fourth order Bessel filter (low pass) and digitized at 0.1-msec intervals. Analysis was done by PDP 11-24 and PDP 11-40 computers (Digital Equipment Corp.) using a maximum zero-crossing algorithm to estab-

lish baselines and channel amplitudes (22). A channel opening was counted when the current was greater than 50% of, or within 4 SD of, the estimated average channel current (these two alternative opening criteria did not noticeably alter the lifetime data). After an opening, the channel was considered to be closed when the current decreased to less than 50% of the mean channel current. At low membrane potentials, when the mean open current was less than 8 SD, lifetimes were not evaluated. Open events which occurred without interruption were analyzed for channel lifetime. When closures of less than 8 msec occurred between openings, the openings were considered to be part of a burst. Short events could not be counted with confidence because the maximum amplitude of events of less than 0.3 msec was reduced by the filtering and the accuracy of timing was limited by digitization. Therefore, the corrected mean lifetime was determined as the mean duration of events 0.5 msec and longer corrected by −0.5 msec (23). The τ value was also estimated using unweighted least squares fitting of a single exponential to the duration histograms. Corrected mean durations and exponentially fitted τ were the same, as expected for stochastic behavior, when applied to burst and open durations. Two populations of closed durations occurred which differed greatly in their mean durations. The duration histograms for closures less than 8 msec were fitted well by single exponential decays, supporting the stochastic nature of the events. The short τ values, however, suggest that many events were undetected; corrected mean durations were not calculated because this would require the assumption of nearly as many events as those actually observed. Because the durations of longer closures depend upon the number of channels in various patches, combined analysis of closures longer than 0.8 msec was not done.

Results

Potency for contracture. The assay of agonist potency by contracture demonstrated that (+)AnTX is 110 (95% confidence range 85–143) times more potent than Carb, whereas (−)AnTX is slightly less potent than Carb (0.74 times, range 0.5–1.0) (Fig. 2). After complete cholinesterase inhibition by the organophosphate DFP, ACh was 14 (range 9–20) times more potent than Carb. ACh was equipotent to Carb when cholinesterase was not inhibited. In the rectus abdominis it appears that (+)AnTX is 8 times more potent than ACh after DFP treatment.

Receptor binding interactions. ACh, (+)AnTX, and (−)AnTX completely inhibited the specific binding of [^{125}I]BGT to the nicotinic receptor in *Torpedo* electric organ (Fig. 3). (+)AnTX (IC_{50} = 0.085 μM; Table 1) was 3-fold more potent in inhibiting [^{125}I]BGT binding than ACh and 50-fold more potent than (−)AnTX.

Ion channel activation effects. All three agonists stimulated the binding of 2 nM [^{3}H]H_{12}-HTX to sites associated with the receptor-gated ion channel (Fig. 4). The maximum degree of stimulation (approximately 50%) was the same with each compound and was obtained at a concentration of 10 μM. At higher concentrations, [^{3}H]H_{12}-HTX binding was depressed (data not shown), perhaps due to competing desensitizing processes (see below). The relative potency of the three agonists at stimulating ion channel binding was in close agreement with their potency at inhibiting [^{125}I]BGT binding to the receptor, suggesting that their influence on ion channel binding is a consequence of their occupancy of receptor-binding sites.

Binding to ionic channel sites. The mechanism for (+)AnTX, (−)AnTX, and ACh stimulation of [^{3}H]H_{12}-HTX binding is illustrated in Fig. 5. At 10 μM, ACh, (+)AnTX, and (−)AnTX all increased [^{3}H]H_{12}-HTX binding affinity to the

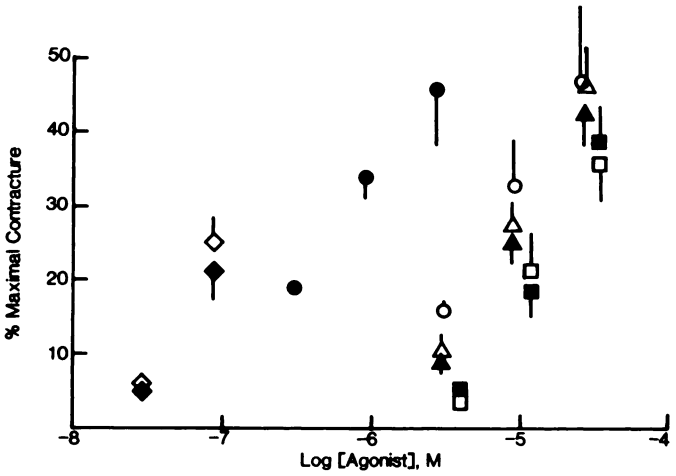

Fig. 2. Relative potency of the (+)- and (−)-isomers of AnTX in eliciting contracture of frog rectus abdominis. The relative potency of agonists to contract the rectus abdominus muscle was determined without (*open symbols*) and with (*solid symbols*) DFP treatment. The relative potency of Carb (△, ▲) and ACh (○, ●) was determined using four muscles each. The relative potencies of Carb, (+)AnTX (◇, ◆), and (−)AnTX (□, ■) were determined using three muscles each. The data presented for Carb represent combined experiments.

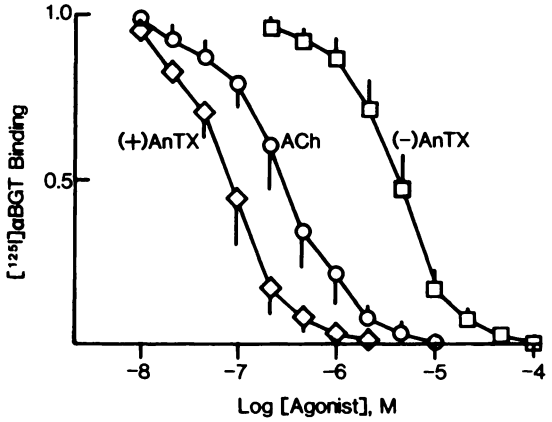

Fig. 3. Interaction of AnTX and ACh with nicotinic receptors from *Torpedo* electric organ. The binding of 5 nM [^{125}I]BGT was measured in the presence of the indicated concentrations of (+)AnTX, (−)AnTX, or ACh. Binding is expressed as the fraction of specific binding measured in the absence of competing ligands. Each *point* and *bar* represent the mean and standard deviation from four experiments.

TABLE 1

Influence of (+)AnTX, (−)AnTX, and ACh on ligand binding to receptor and ion channel sites in Torpedo electric organ

Compound	Receptor [^{125}I]BGT		Ion channel [^{3}H]H_{12}-HTX	
	IC_{50}[a]	R^b	ED_{50}[c]	R^b
	μM		μM	
ACh	0.30 ± 0.05[d]	1	0.15 ± 0.06	1
(+)AnTX	0.085 ± 0.008	3.5	0.032 ± 0.10	4.7
(−)AnTX	4.4 ± 0.3	0.068	1.6 ± 0.3	0.094

[a] The concentration of agonist which inhibited 5 nM [^{125}I]BGT binding by 50% under the assay conditions described in Materials and Methods.

[b] Relative potency of the agonists compared to ACh at inhibiting receptor binding and stimulating ion channel binding.

[c] The concentration of agonist which stimulated the binding of 2 nM [^{3}H]H_{12}-HTX to half of the maximal extent. All of the agonists stimulated [^{3}H]H_{12}-HTX binding to the same extent (about 50%).

[d] Values are means ± standard deviation, N = 4 in each case.

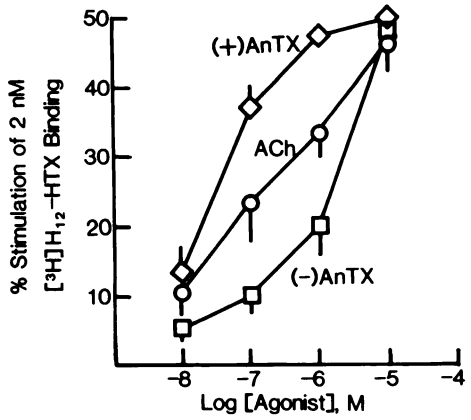

Fig. 4. Stimulation of ion channel binding by AnTX and ACh. The binding of 2 nM [^{3}H]H_{12}-HTX and the indicated concentration of (+)AnTX, (−)AnTX, or ACh to a suspension of membranes prepared from *Torpedo* electric organ is shown. Binding is expressed as the percentage increase in binding relative to that measured in the absence of a receptor agonist. Each *point* and *bar* represent the mean and standard deviation from four separate experiments.

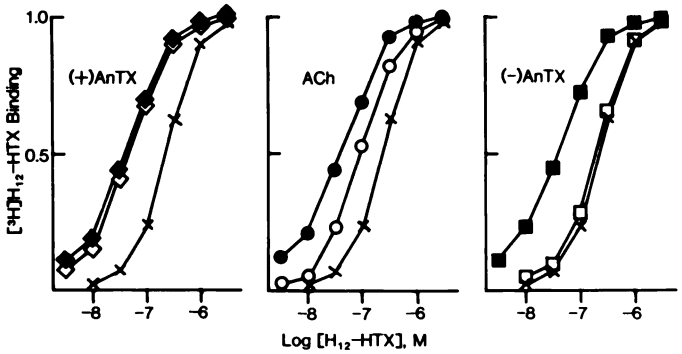

Fig. 5. Influence of AnTX and ACh on the affinity of H_{12}-HTX for ion channel binding sites. [^{3}H]H_{12}-HTX binding, expressed as fractional receptor occupancy, was determined in competition studies using 2nM [^{2}H]H_{12}-HTX. Binding curves were obtained in the absence (*X*) or presence of 0.1 μM (*open symbols*) and 10 μM (*solid symbols*) (+)AnTX, ACh, or (−)AnTX. Each *point* represents the mean from three experiments which varied by less than 15% at all levels of receptor occupancy.

same extent (6-fold, from 0.23 to 0.039 μM). (+)AnTX was equally effective at 0.1 and 10 μM, whereas (−)AnTX was ineffective at 0.1 μM and ACh had an intermediate effect at 0.1 μM. This is in good agreement with the potency of the agonists at inhibiting [^{125}I]BGT binding and stimulating non-equilibrium [^{3}H]H_{12}-HTX binding (Figs. 3 and 4, Table 1).

Desensitization. Preincubation of *Torpedo* membranes with (+)AnTX or ACh decreased their stimulation of [^{3}H]H_{12}-HTX binding in a time-dependent fashion (Fig. 6). After a 10-min preincubation with 10 μM (+)AnTX or ACh, no stimulation of [^{3}H]H_{12}-HTX binding was observed. The time courses for the development of this "desensitization" was different with (+)AnTX and ACh. Despite its higher affinity for the receptor, at equal agonist concentrations the onset of (+)AnTX-induced desensitization was delayed compared to the onset of ACh-induced desensitization. At 10 μM, desensitization was 50% complete after a 1.7-min preincubation with ACh but only after a 3-min incubation with (+)AnTX (Fig. 6). Similar differences between ACh and AnTX desensitization were observed when using lower concentrations (0.1 and 1 μM) of the agonists. For example, desensitization was 50% complete after 3.5 min with 1 μM ACh, but only after 4.5 min with 1 μM AnTX.

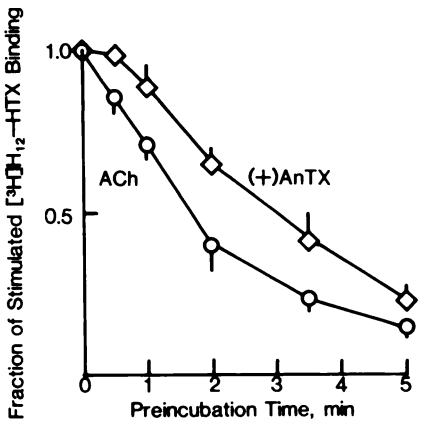

Fig. 6. Time course of desensitization induced by ACh and (+)AnTX. *Torpedo* membranes were incubated with 10μM ACh or (+)AnTX for the time indicated on the *abscissa*. [^{3}H]H_{12}-HTX was then added (final concentration of 2 nM) and binding was determined by filtration 60 sec later. Binding is expressed as a fraction of stimulated binding measured after the simultaneous addition of [^{3}H]H_{12}-HTX and ACh or (+)AnTX. ACh and (+)AnTX stimulated [^{3}H]H_{12}-HTX binding to the same maximal extent (approximately 50%). Each *point* and *bar* represent the mean and standard deviation from four experiments.

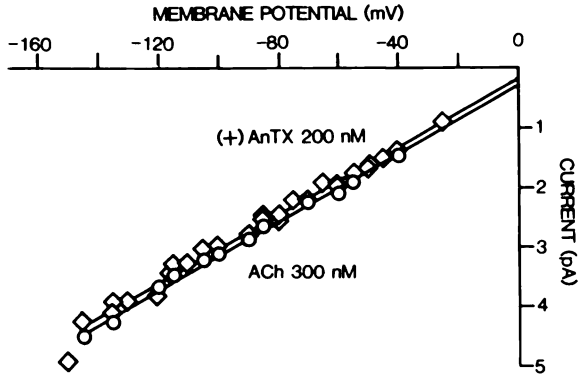

Fig. 7. Conductance of single ACh ionic channels. The slope conductances for 200 nM (+)AnTX and 300 nM ACh were found to be the same in several patches. Each *point* on an *I-V* line is the current in one patch at that potential; for ACh (O), three patches were found on three cells, and for (+)AnTX (◇), five patches on four cells were found.

Single channel conductance. Single currents sampled from cell-attached patches were recorded using either ACh or AnTX in the microelectrodes. Whenever possible, recordings using both agonists were obtained from the same cell, but when this was not feasible, recordings were done using fibers isolated on the same day. The slope conductance of ACh and (+)AnTX-activated channels was the same (Fig. 7), i.e., for ACh (300 nM) the channel conductance was 27.4 ± 1.4 pS (mean ± SD for individual determinations from five to seven patches), and the current at −90 mV was 3.0 ± 0.3 pamp. In the case of (+)AnTX, values were 28.9 ± 4.9 and 28.7 ± 1.7 pS for 20 and 200 nM, respectively. The current recorded at −90 mV was 2.5 ± 0.3 pamp in the presence of 20 nM (+)AnTX and 2.8 ± 0.1 pamp at a 200 nM concentration of the toxin. The reversal potentials for both ACh and (+)AnTX were similar.

Lifetime kinetics. Characteristic ACh and (+)AnTX-activated channels are shown in Fig. 8. Although both (+)AnTX and (−)AnTX were at least 99.95% pure, (−)AnTX induced a low frequency of channel openings even at concentrations above 800 μM. Accordingly, patch clamp experiments using

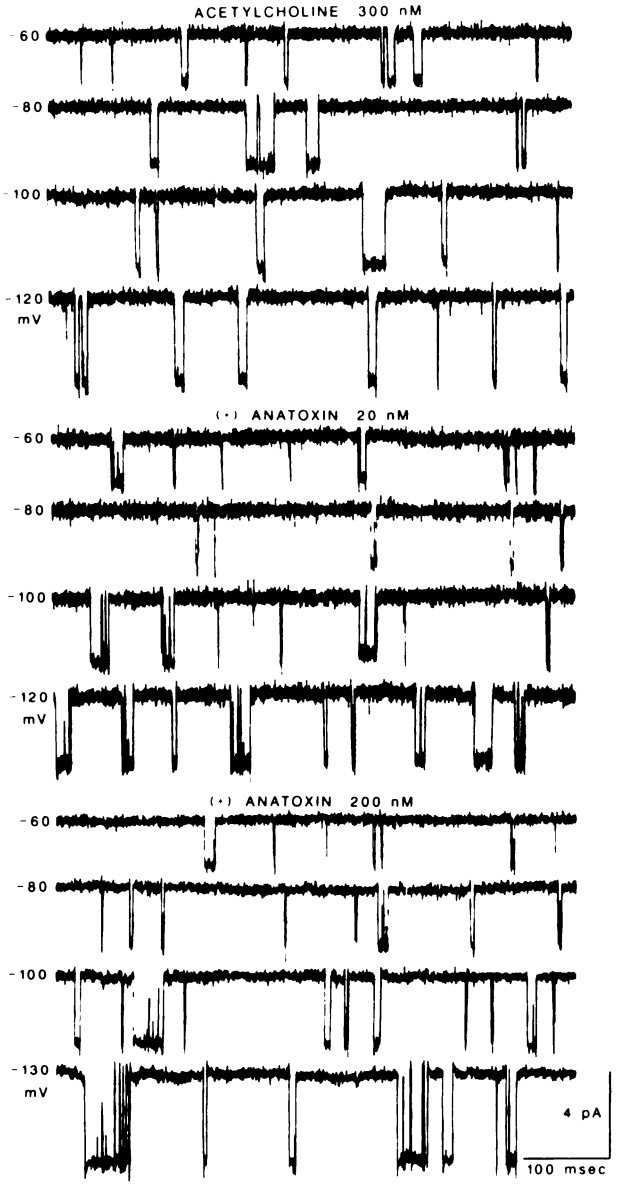

Fig. 8. Single channel currents induced by ACh and (+)AnTX. Current recordings at several transmembrane potentials are shown with ACh (300 nM) and (+)AnTX (20 and 200 nM) as the agonists. At hyperpolarized potentials the channels remained open longer. The channels shown are typical with respect to the number of short closing events. With ACh there were few short closing events. The toxin-induced channels are very similar to those seen with ACh except for the greater number of short closures. The number of closures within bursts does not increase with lengthening of the burst.

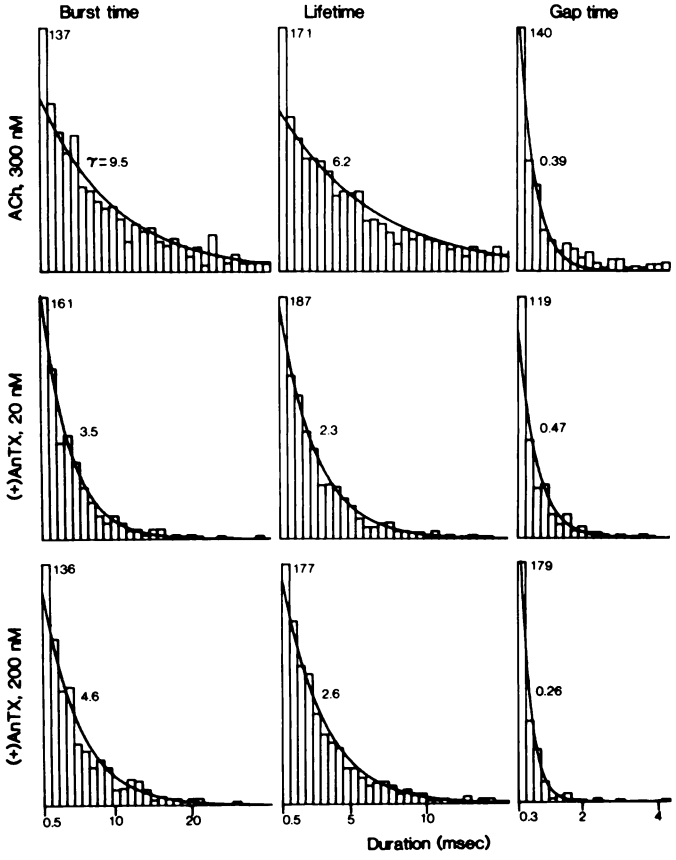

Fig. 9. Distribution of durations used in stochastic analysis. Histograms of channel burst, open, and gap (short closed) durations are shown in each *column*. Comparison of the effects of ACh (300 nM) and AnTX (20 and 200 nM) shows little difference between the concentrations of AnTX in rows 2 and 3, but AnTX burst and open durations are shorter than those of ACh in row 1. In column 3, the distribution of the short closures show no difference between agonists.

(−)AnTX were not pursued further. The channels activated by (+)AnTX resembled those induced by ACh but had short interruptions of the channel current. The duration of closed states was distributed biexponentially for both ACh and (+)AnTX, with the short and long phases well separated by the 8-msec cutoff (Fig. 9). Short-duration closed states were relatively infrequent with ACh but numerous with (+)AnTX.

The mean duration of bursts was distributed according to a single exponential function with both ACh and (+)AnTX as the agonist (Fig. 9). The burst duration of both ACh- and (+)AnTX-activated channels increased *e*-fold for 50–60 mV hyperpolarization (Table 2, Fig. 10). The duration of (+)AnTX bursts was shorter than that of ACh bursts at all membrane potentials tested. For example, the mean channel burst duration at −90 mV membrane potential was 9 msec for the ACh-evoked channel openings and 5 msec for the AnTX-evoked openings (Table 2).

The lifetime of channels opened by ACh was only slightly shorter than their burst time (Fig. 10), whereas the lifetime of channels opened by (+)AnTX was approximately one-half of the (+)AnTX burst time (Table 2). At all membrane potentials tested, the (+)AnTX lifetime was a constant fraction of the burst time; thus, the semilogarithmic plots of mean duration of burst times and lifetimes versus membrane potential were parallel (Fig. 10). This may be attributed to the division of the activated phase (burst) of each channel into openings separated by short closures. This is emphasized at hyperpolarized potentials, where, in spite of the longer burst duration, the number of short closures caused by (+)AnTX within each burst seems to be constant. The frequency of short closures during bursts is, therefore, less.

The durations of short closing events with both ACh and (+)AnTX, estimated by τ as described in detail in Materials and Methods, were approximately 0.4 msec at all potentials (Fig. 10). Although this value approaches the limit of detection, the exponentially fitted τ would easily have shown longer mean durations if they had occurred. This suggests that the gap duration induced by AnTX was voltage independent, as re-

TABLE 2

Kinetic properties of nicotinic ionic channels of frog skeletal muscle in response to ACh and AnTX

Agonist	Concentration	Lifetime at −90 mV	e-fold	Burst time at −90 mV	e-fold
	nM	*msec*	*mV*	*msec*	*mV*
ACh	300	6.7 (5.7–8.0)[a]	63 (48–89)	8.9 (7.7–10.0)	56 (45–73)
(+)AnTX	20	2.9 (2.4–3.3)	57 (47–76)	4.8 (4.3–5.4)	49 (43–58)
(+)AnTX	200	2.7 (2.4–2.9)	84 (69–106)	5.3 (4.7–6.0)	63 (52–82)

[a] Ranges are 95% confidence intervals, n = 17–22 potentials for each fit line.

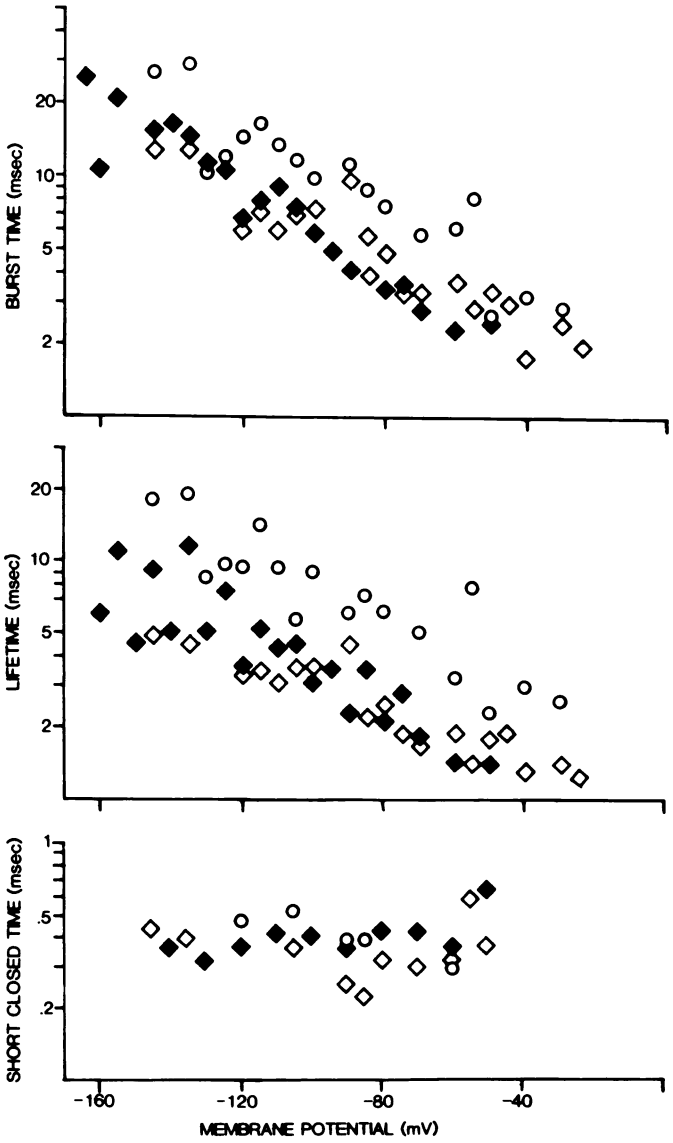

Fig. 10. Durations of channel states dependent upon membrane potential. The average lifetimes, burst times, and closed times are plotted as a function of membrane potential. The voltage dependence was determined using 300 nM ACh (○), 20 nM (◆), and 200 nM (◇) (+)AnTX. With ACh, the mean lifetimes are slightly, but not significantly, shorter than the burst times. With either 20 or 200 nM (+)AnTX, the lifetimes are a constant fraction of the burst time, representing a constant rate of rapid closures occurring during the open phase. The standard errors of the values were not shown for clarity.

ported for gap durations for other agonists (24), although uncertainty remains because of large relative standard errors. It has also been suggested that the duration of agonist-induced gaps is voltage dependent (25). Because events shorter than 0.2 msec were less than 50% amplitude (with filtering at 2 KHz and digitization at 0.1 msec), the number of closures observed within a burst was probably 60% or less than the actual number of closures which occurred, and the duration of open times was overestimated (Table 2). If the apparently stochastic behavior is assumed and the occurrence of closed durations less than 0.2 msec is calculated, one predicts that, with (+)AnTX, there would actually be one closure within each burst, and that the lifetime of the channel is actually 5.6 msec for ACh and 2–2.3 msec for (+)AnTX.

The duration of the burst time and lifetime did not change as the concentration of (+)AnTX was increased from 20 to 200 nM. The frequency of fast closures also was the same at 20 and 200 nM (+)AnTX, as indicated by the similar ratio of open time to burst time. The concentration-independent effect of (+)AnTX on short channel closures is fundamental to the toxin's mechanism of action.

Desensitization. At high concentrations, (±)AnTX caused desensitization of the ACh receptor ion channel (6). In patch clamp experiments, 800 nM (+)AnTX caused an initially high frequency of channel openings with few simultaneous multiple openings, after the seal was established, which decreased over 1 or 2 min and stopped abruptly. Subsequently isolated bursts of high frequency activity, each beginning and terminating abruptly, appeared following long inactive intervals. The high frequency of events appears to be due to repetitive opening of a single channel because simultaneous opening of more than one channel did not occur within these bursts. In spite of the high frequency of activity observed with high (+)AnTX concentration (800 nM), the channel conductance and lifetimes were not altered.

Discussion

(+)AnTX acts as a potent nicotinic agonist to elicit muscle contracture (Fig. 2) and is about 8 times more potent than ACh after AChE inhibition. This potency was largely due to a 3.6-fold greater affinity for the agonist-binding site on the nicotinic receptor. Binding of two agonist molecules to α-chains of the receptor are required to activate a single channel (26, 27). If there is no allosteric cooperativity, the fraction of doubly liganded sites is the square of the fraction of sites bound,[3] so that 13 times more receptors would be doubly liganded with

[3] For a ligand binding to a single site according to $R_0 + A = R_1$, the dissociation constant is $K = ([A] \times R_0)/R_1$. For n homologous sites without cooperativity, $R_1 = n\ R_0\ [A]/K$ and $R_2 = ((n-1)/2)\ R_1\ [A]/K$. In the present case of $n = 2$, this reduces to $R_1 = 2R_0\ [A]/K$ and, with appropriate substitutions, $R_2 = R_0\ ([A]/K)^2$. The fraction of doubly liganded sites is $Y_2 = R_2/(R_0 + R_1 + R_2)$; by allowing the simplifying term $\alpha = [A]/K$, then $Y_2 = \alpha^2/(1 + \alpha)^2$. The fraction of all sites bound is $Y_A = (R_1 + 2R_2)/2(R_0 + R_1 + R_2)$, which, with the appropriate substitutions and simplification, yields $Y_A = \alpha/(1 + \alpha)$ [also in accordance with the rule of $Y_A = \alpha(1 + \alpha)^{n-1}/(1 + \alpha)^n$ at $n = 2$). Therefore, the fraction of doubly bound receptors, Y_2, is the square of the fraction of all sites bound, Y_A (28).

(+)AnTX than with ACh (28). This is slightly greater than the observed contracture potency ratio. Therefore, the high potency of (+)AnTX activity may be accounted for by its higher binding affinity (see Fig. 3) which elicits channel opening and increases histrionicotoxin binding affinity. The relative potency of (+)- and (−)AnTX for contracture is at least 150-fold, much greater than previously noted for nicotinic agonists. [(−)Nicotine has only 8-fold more potency than (+)nicotine (10).] Because (−)AnTX has only a small fraction of the potency of (+)AnTX, it is possible that some of the observed pharmacological action of (−)AnTX is due to a minor contaminant of (+)-isomer in the sample (3).

This study demonstrated that channel conductance is similar with (+)AnTX and ACh, in contrast to the previous report that conductance was reduced 25% by (±)AnTX as measured by fluctuation analysis (6). Similar discrepancies between fluctuation analysis and single channel studies have also been encountered in other laboratories (Ref. 29 versus Refs. 25, 30). Three apparent sources of error in the previous AnTX study are from filtering, high agonist concentration, and stimulation of ACh release by the toxin. In noise analysis, the filtering (800 Hz) limits the detection of events to those with mean durations greater than 1.3 msec. Therefore, some of the more brief AnTX-activated channels, observed in patch experiments, may have been attenuated in amplitude. Another error could arise from assuming that the probability of channel opening, p, is very small and, therefore, neglecting p in the equation $\sigma^2/\mu = \gamma n(1-p)$, resulting in a lower conductance estimate. With a high concentration of (±)AnTX, most receptors would be bound and the ionic channels would be open most of the time, so that (+)AnTX-induced fluctuations would actually be relatively small. Because the noise analysis was not done with denervated muscles, fluctuations included ACh-activated channels as a consequence of presynaptic ACh release (6). ACh may have even acted as a channel blocker under these conditions (31, 32).

Slower desensitization would enhance the relative potency of AnTX for events, such as muscle contracture, occurring over a period of minutes. Preincubation of *Torpedo* membranes with nicotinic agonists [including (+)AnTX] for a few minutes depresses the binding of ion channel probes such as [^{3}H]H_{12}-HTX. This depression is believed to reflect induction of desensitized receptor conformations (19, 20). It was clear in patch clamp studies that channel activity decreased over a 2-min period at 800 nM (+)AnTX. This confirms that the inhibition of HTX binding occurred through desensitization and not by blocking the ionic channel. This also confirms the previous interpretation that 900 nM (±)AnTX depressed peak end plate current by desensitization and exclusion of receptors (6). Despite the 3.6-fold greater binding of (+)AnTX than of ACh, at 10 μM the onset of desensitization by the toxin occurred at a 2-fold slower rate than with ACh.

A difference between (+)AnTX and ACh-activated channels was an increased frequency of short gaps and a shortened open channel time. The shorter ionic channel burst time for the toxin than for ACh actually decreased the current flow, counteracting the effect higher binding affinity would contribute to contracture potency. (+)AnTX-induced short closures did not have the characteristics of channel blocking induced by local anesthetics or other agents such as mecamylamine (33–35). The frequency of ionic channel blocking is voltage independent but is concentration dependent with certain local anesthetics. The frequency of AnTX gaps, in contrast, was voltage dependent (less frequent at hyperpolarized potentials) and concentration (20–200 nM) independent. The mean duration of channel blockade by local anesthetics was also voltage dependent, but the duration of AnTX gaps was apparently voltage independent. Furthermore, the BGT and H_{12}-HTX binding studies indicated that the toxin binds only to the ACh-binding site and not to sites associated with the ionic channel (19).

The channel properties associated with (+)AnTX stimulation suggest that the toxin causes multiple opening and closing transitions of individual channels and that these transitions are independent of free agonist concentration. The short gaps may represent normal closures of the ionic channel which are followed by reopenings, nachschlags, without dissociation of the agonist from the receptor (35).

$$\textbf{Model 1: } A + R \underset{k_{-1}}{\overset{k_1}{\rightleftharpoons}} AR \underset{k_{-2}}{\overset{k_2}{\rightleftharpoons}} A_2R \underset{\alpha}{\overset{\beta}{\rightleftharpoons}} A_2R^*$$

In Model 1, the number of gaps per burst, $(\beta/2k_{-2})$, is determined by the rate of opening (β) as compared with the combined rates of dissociation of either of two agonist molecules ($2k_{-2}$) which terminate the burst; the lifetime of the doubly liganded closed state is $(\beta + 2k_{-2})^{-1}$ and the lifetime of the open channel is α^{-1} (24). The kinetic parameters derived using this model and the observed data suggest that (+)AnTX dissociates more slowly (700 sec^{-1}) than ACh (960 sec^{-1}) but that the transitions between opened and closed channel states occur more rapidly (Table 3). An alternate possibility is that a closed state exists which is accessible only from the open state,

$$\textbf{Model 2: } A_2R \underset{\alpha}{\overset{\beta}{\rightleftharpoons}} A_2R^* \underset{k_{-3}}{\overset{k_3}{\rightleftharpoons}} A_2R$$

In Model 2, the number of openings per burst, (k_3/α) is the rate of added closure (k_3) compared with the rate of normal closure (α), the lifetime of the open channel is $(\alpha + k_3)^{-1}$, and the duration of the gap is k_3^{-1}. A more complex model with two open states has also been proposed for short-duration gaps (36).

It has been observed previously that several agonists cause these rapid, concentration-independent transitions (25, 36, 37). The transitions differed in number and duration with different agonists. The duration of gaps averaged 20–40 μsec in frog muscle (37) and 300 μsec at snake endplates (25). Our analysis would have missed gaps shorter than 200 μsec. Similar rapid transitions have also been observed in other transmitter-gated channels (37). Therefore, we suggest that the origin of the transition lies in the receptor-channel macromolecule and the agonists modulate it.

Even though AnTX is structurally more rigid than ACh, it does have destabilizing properties. Intramolecular hydrogen bonding may encourage movement between the *s-cis* and *s-trans* conformations (1). In physiological solution it is probably

TABLE 3
Kinetics parameters of the receptor-ionic channel complex

Agonist	Model 1			Model 2		
	k_{-2}	β	α	α	k_3	k_{-3}
ACh	961[a]	577	200	87	113	2500
AnTX	694	1111	400	142	255	2500

[a] Values are estimated rate constants in sec^{-1} based on mean values reported in Table 2.

protonated (+)AnTX that binds to the receptor and activates the ionic channel (as suggested for tertiary muscarinic agonists; Ref. 38), and proton dissociation may enhance channel closure. Because active tissue is sensitive to pH (39, 40), the H^+-dependent properties of non-quaternary amine agonists and the nicotinic receptor deserve further investigation. The greater rigidity of (+)AnTX may be responsible for the greater rate of closure. During ionic channel activation, conformational changes of the receptor macromolecule may be accommodated by the flexibility of many agonists. In contrast, the rigidity of (+)AnTX would destabilize the open conformation.

In summary, (+)AnTX is a stereospecific nicotinic agonist whose potency depends upon high affinity binding to the nicotinic receptor-ionic channel complex and relatively less desensitization than ACh. The conductance of the channels is the same with both agonists. Ionic currents of single channels activated by (+)AnTX are, however, shorter than those induced by ACh. The toxin does not bind to ionic channel sites. Because ionic channel activation is independent of desensitization, it may also be possible to develop agonists with greater relative stability for various ionic channel conformations.

Acknowledgments

We thank Ms. Mabel A. Zelle for her assistance with analysis of the single channel data. We are grateful to Dr. John W. Daly, Chief of the Laboratory of Bioorganic Chemistry, National Institute of Arthritis, Diabetes and Digestive and Kidney Diseases, National Institutes of Health, for providing the [^{3}H] perhydrohistrionicotoxin used in these studies.

References

1. Huber, C. S. The crystal structure and absolute configuration of 2,9-diacetyl-9-azabicyclo[4,2,1]non-2,3-ene. *Acta Crystallogr. Sect. B Struct. Crystallogr. Cryst. Chem.* **28**:2577–2582 (1972).
2. Devlin, J. P., O. E. Edwards, P. R. Gorham, H. R. Hunter, R. K. Pike, and B. Stavric. Anatoxin-a, a toxic alkaloid from *Anabeana flos-aquae* NRC-44h. *Can. J. Chem.* **55**:1367–1371 (1977).
3. Koskinen, A. M. P., and H. Rapoport. Synthetic, conformational and pharmacological studies of anatoxin-a, a potent acetylcholine agonist. *J. Med. Chem.* **28**:1301–1309 (1985).
4. Carmichael, W. W., D. F. Biggs, and P. R. Gorham. Toxicology and pharmacological action of *Anabaena flos-aquae* toxin. *Science (Washington. D. C.)* **187**:542–544 (1975).
5. Carmichael, W. W., D. F. Biggs, and M. A. Peterson. Pharmacology of Anatoxin-a, produced by the freshwater cyanophyte *Anabaena flos-aquae* NRC-44-1. *Toxicon* **17**:229–236 (1979).
6. Spivak, C. E., B. Witkop, and E. X. Albuquerque. Anatoxin-a: a novel, potent agonist at the nicotinic receptor. *Mol. Pharmacol.* **18**:384–394 (1980).
7. Aronstam, R. S., and B. Witkop. Anatoxin-a interactions with cholinergic synaptic molecules. *Proc. Natl. Acad. Sci. USA* **78**:4639–4643 (1981).
8. Spivak, C. E., and E. X. Albuquerque. Dynamic properties of the nicotinic acetylcholine receptor ionic channel complex: activation and blockade, in *Progress in Cholinergic Biology: Model Cholinergic Synapses* (I. Hanin and A. M. Goldberg, eds.). Raven Press, New York, 323–357 (1982).
9. Beers, W. H., and E. Reich. Structure and activity of acetylcholine. *Nature (Lond.)* **288**:917–922 (1970).
10. Chothia, C., and P. Pauling. The conformation of cholinergic molecules at nicotinic nerve receptors. *Proc. Natl. Acad. Sci. USA* **65**:477–482 (1970).
11. Spivak, C. E., J. Waters, B. Witkop, and E. X. Albuquerque. Potencies and channel properties induced by semirigid agonists at frog nicotinic acetylcholine receptors. *Mol. Pharmacol.* **23**:337–343 (1983).
12. Albuquerque, E. X., and C. E. Spivak. Natural toxins and their analogues that activate and block the ionic channel of the nicotinic acetylcholine receptor, in *Natural Products and Drug Development, Alfred Benson Symposium 20* (P. Krogsgaard-Larsen, S. Brogger Christensen, and H. Hofod, eds.). Munksgaard, Copenhagen, 301–323 (1984).
13. Roger, A. W., Z. Darzynkiewicz, M. M. Salpeter, K. Ostrowski, and E. A. Barnard. Quantitative studies on enzymes in structures in striated muscles by labeled inhibitor methods. *J. Cell Biol.* **41**:665–685 (1969).
14. Kuba, K., E. X. Albuquerque, J. Daly, and E. X. Barnard. A study of the irreversible cholinesterase inhibitor, diisopropylfluorophosphate on time course of endplate currents in frog sartorius muscle. *J. Pharmacol. Exp. Ther.* **189**:499–512 (1974).
15. Colquhoun D. *Lectures on Biostatistics*. Clarendon Press, Oxford, 279–343 (1971).
16. Lowry, O. H., N. J. Rosebrough, A. L. Farr, and R. J. Randall. Protein measurement with the Folin phenol reagent. *J. Biol. Chem.* **193**:265–275 (1951).
17. Aronstam, R. S., C. T. King, E. X. Albuquerque, J. W. Daly, and D. M. Feigl. Binding of [^{3}H]perhydrohistrionicotoxin and [^{3}H]phencyclidine to the nicotinic receptor ion channel complex of *Torpedo* electroplax: inhibition by histrionicotoxins and derivatives. *Biochem. Pharmacol.* **34**:3037–3047 (1985).
18. Albuquerque, E. X., M.-C. Tsai, R. S. Aronstam, B. Witkop, A. T. Eldefrawi, and M. E. Eldefrawi. Phencyclidine interactions with the ionic channels of the acetylcholine receptor and electrogenic membrane. *Proc. Natl. Acad. Sci. USA* **77**:1224–1228 (1980).
19. Aronstam, R. S., A. T. Eldefrawi, I. N. Pessah, J. W. Daly, E. X. Albuquerque, and M. E. Eldefrawi. Regulation of [^{3}H]perhydrohistrionicotoxin binding to *Torpedo ocellata* electroplax by effectors of the acetylcholine receptor. *J. Biol. Chem.* **256**:2843–2850 (1981).
20. Oswald, R. E., T. Heidmann, and J.-P. Changeux. Multiple affinity states for noncompetitive blockers revealed by [^{3}H]phencyclidine binding to acetylcholine receptor rich membrane fragments from *Torpedo marmorata*. *Biochemistry* **22**:3128–3136 (1983).
21. Allen, C. N., A. Akaike, and E. X. Albuquerque. The frog interosseal muscle fiber as a new model for patch clamp studies of chemosensitive and voltage-sensitive ion channels: actions of acetylcholine and batrachotoxin. *J. Physiol. (Paris)* **79**:338–343 (1984).
22. Sachs, F., J. Neil, and N. Barkakati. The automated analysis of data from single ion channels. *Pfluegers Arch. Eur. J. Physiol.* **395**:331–340 (1982).
23. Colquhoun, D., and F. J. Sigworth. Fitting and statistical analysis of single-channel records, in *Single Channel Recording* (B. Sakmann and E. Neher, eds.). Plenum Press, New York, 191–263 (1983).
24. Colquhoun, D., and B. Sakmann. Fluctuation in the microsecond time range of the current through single acetylcholine receptor ion channels. *Nature (Lond.)* **294**:464–466 (1981).
25. Leibowitz, M. D., and V. E. Dionne. Single channel acetylcholine receptor kinetics. *Biophys. J.* **45**:153–162 (1984).
26. Magleby, K. L., and C. F. Stevens. A quantitative description of end-plate currents. *J. Physiol. (Lond.)* **223**:173–197 (1972).
27. Adler, M., E. X. Albuquerque, and F. J. Lebeda. Kinetic analysis of end plate currents altered by atropine and scopolamine. *Mol. Pharmacol.* **14**:514–529 (1978).
28. Monod, J., J. Wyman, and J. P. Changeux. On the nature of allosteric transitions: a plausible model. *J. Mol. Biol.* **12**:88–118 (1965).
29. Colquhoun, D., V. E. Dionne, J. H. Steinbach, and C. E. Stevens. Conductance of channels opened by acetylcholine-like drugs in muscle end-plate. *Nature (Lond.)* **253**:204–206 (1975).
30. Gardner, P., D. C. Ogden, and D. Colquhoun. Conductance of single ion channels opened by nicotinic agonists are indistinguishable. *Nature (Lond.)* **309**:160–162 (1984).
31. Adams, P. R., and B. Sakmann. A comparison of current-voltage relations for full and partial agonists. *J. Physiol. (Lond.)* **283**:621–644 (1978).
32. Adams, D. J., and D. Colquhoun. Current relaxations with high agonist concentrations. Do acetylcholine and suberyldicholine block ion channels in frog muscle? *J. Physiol. (Lond.)* **341**:22P (1983).
33. Neher, E., and J. H. Steinbach. Local anaesthetics transiently block currents through single acetylcholine-receptor channels. *J. Physiol. (Lond.)* **277**:153–176 (1978).
34. Aracava, Y., S. R. Ikeda, J. W. Daly, N. Brookes, and E. X. Albuquerque. Interactions of bupivacaine with ionic channels of the nicotinic receptor: analysis of single-channel currents. *Mol. Pharmacol.* **26**:304–313 (1984).
35. Varanda, W. A., Y. Aracava, S. M. Sherby, W. B. VanMeter, M. E. Eldefrawi, and E. X. Albuquerque. The acetylcholine receptor of the neuromuscular junction recognizes mecamylamine as a noncompetitive antagonist. *Mol. Pharmacol.* **28**:128–137 (1985).
36. Sine, S. M., and J. H. Steinbach. Activation of a nicotinic acetylcholine receptor. *Biophys. J.* **45**:175–185 (1984).
37. Colquhoun, D., and B. Sakmann. Bursts of openings in transmitter-activated ion channels, in *Single-Channel Recording* (B. Sakmann and E. Neher, eds.). Plenum Press, New York, 345–364 (1983).
38. Ehlert, F. J., and D. J. Jenden. Comparison of the muscarinic receptor binding activity of some tertiary amines and their quaternary ammonium analogues. *Mol. Pharmacol.* **25**:46–50 (1984).
39. Spray, D. C., R. L. White, A. Campos de Carvalho, A. L. Harris, and M. V. L. Bennett. Gating of gap junction channels. *Biophys. J.* **45**:219–230 (1984).
40. Roberts, E., Z. Liron, E. Wong, and F. Schroeder. Roles of proton removal and membrane fluidity in Na^+ and Cl^--dependent uptake of γ-aminobutyric acid by mouse brain particles. *Exp. Neurol.* **88**:13–26 (1985).

Send reprint requests to: Dr. E. X. Albuquerque, Department of Pharmacology and Experimental Therapeutics, University of Maryland School of Medicine, 655 West Baltimore Street, Baltimore, MD 21201.